Ore Geology Reviews 87 (2017) 147–154

Contents lists available at ScienceDirect

Ore Geology Reviews

journal homepage: www.elsevier.com/locate/oregeorev

Sulfide geochronology along the Northern Equatorial Mid-Atlantic Ridge

Georgy Cherkashov [a,b,*], Vladislav Kuznetsov [b], Katherine Kuksa [b], Erik Tabuns [b], Fedor Maksimov [b], Victor Bel'tenev [c]

[a] Institute for Geology and Mineral Resources of the Ocean (VNIIOkeangeologia), Angliysky Avenue 1, 190121 St. Petersburg, Russia
[b] St. Petersburg State University, 7/9 Universitetskaya nab., 199034 St. Petersburg, Russia
[c] Polar Marine Geosurvey Expedition, Pobedy Str. 24, Lomonosov, 198412 St. Petersburg, Russia

ARTICLE INFO

Article history:
Received 21 April 2016
Received in revised form 11 October 2016
Accepted 14 October 2016
Available online 19 October 2016

Keywords:
Mid-Atlantic Ridge
Hydrothermal activity
Seafloor massive sulfides
^{230}Th/U dating

ABSTRACT

Hydrothermal processes and seafloor massive sulfide (SMS) deposits have different characteristics at fast and slow spreading mid-ocean ridges. One such parameter is the age of a SMS deposit, which differs by 1–2 orders of magnitude between the fast spreading East Pacific Rise (EPR) and the slow spreading Mid-Atlantic Ridge (MAR). The large collection of SMS samples dated from the 18 hydrothermal fields of the northern equatorial part of the Mid-Atlantic Ridge (194 samples) demonstrates a relatively old average age of hydrothermal fields here (~66 ka) with the oldest one estimated as ca. 223 ka (Peterburgskoye field). Based on geochronological data it was confirmed that hydrothermal discharge has an episodic character: active and inactive periods of the SMS formation alternate. The distribution of events at all hydrothermal fields demonstrates that maximum activity occurred at 38–35, 30–20, and 8–2 ka and increased with time. Based on statistical analyses, dating variations can be explained as a superposition of several periods of activity with the duration of ~15, 10 and 5 ka. Relationship between the age and distance from the axial rift zone as well as between the age and aerial distribution is different for SMS deposits hosted by basalts and by gabbro-peridotites depending on their geological setting on the particular MAR segment. This difference can be explained by a variety of hydrothermal processes determined by "tectonic" or "magmatic" segment evolution and symmetrical or asymmetrical mode of accretion (Escartin et al., 2008).

1. Introduction

Seafloor massive sulfides (SMS) are considered modern analogues of land-based volcanogenic massive sulfide (VMS) deposits which formed over the entire history of our planet from the Archean to the present (Hannington et al., 2005; Franklin et al., 2005).

The age (onset time of sulfide deposit formation) and the longevity (lifespan) of the mineral accumulation process should be distinguished because they represent two different important parameters required to understand the evolution of the hydrothermal system. The isotope geochronological methods used for VMS dating (primarily Re/Os) enable the assessment only of the onset time of mineral formation. The longevity of VMS formation remains unknown because the duration of the mineral-forming process and the age of the deposits are not comparable. It is true that in VMS, the duration can at least have maximum bounds established based on dating footwall and hanging wall rocks. However, the precision of K/Ar, Re/Os and other dating methods of the ancient rocks has a rather rough character.

The discovery and study of modern SMS deposits made it possible to considerably fill the gaps in the knowledge of ore-forming process evolution. First, direct observations and monitoring of black smokers activity became accessible. The last growth of a sulfide chimney measured in days-weeks-months and years was recorded in hydrothermal fields for example on the Juan de Fuca Ridge: one sulfide chimney grew up to 1.2 m during one day (Delaney et al., 1990); another 10 m high edifice formed over a year (Kelley et al., 2012). Second, apart from direct observation, isotope analysis of modern oceanic mineral deposits allows us to reconstruct the hydrothermal activity process over a time interval of 10 to 10^5 years. This method is the same as that used for ancient ores and rocks. However, unlike the ancient VMS, short-lived (from years to several hundred thousand years) U-series ^{230}Th, ^{226}Ra and ^{210}Pb isotopes are used for dating modern sulfides based on ^{230}Th/U, ^{226}Ra/Ba and ^{210}Pb/Pb ratios, which make the geochronological study considerably more precise. Seafloor massive sulfides are usually dated by the ^{230}Th/U method reaching in age back to ~350 ka; the younger ages are determined also by the ^{210}Pb/Pb and ^{226}Ra/Ba methods (from 0 to 110 and 200 to 20,000 years, respectively).

The dating of modern seafloor massive sulfides followed their discovery in the end of the 1970s. The first age data were determined in the 1980s for samples from the Pacific (East Pacific Rise) (Lalou and

* Corresponding author at: VNIIOkeangeologia, 1 Anglisky Avenue, St. Petersburg 190121, Russia.
E-mail address: gcherkashov@gmail.com (G. Cherkashov).

http://dx.doi.org/10.1016/j.oregeorev.2016.10.015
0169-1368/

Brichet, 1982) and later from the Atlantic (Mid-Atlantic Ridge) (Lalou et al., 1990, 1993) and Indian Ocean (Southwest Indian Ridge) (Munch et al., 2001; Wang et al., 2012; Lalou et al., 1998a,b). Even later, sulfide dating was carried out on samples from intraoceanic arcs (de Ronde et al., 2011; Ditchburn et al., 2012) and then from the Juan de Fuca Ridge (Jamieson et al., 2013).

The dating of modern oceanic sulfides has both fundamental (understanding evolution of the Earth) and applied/exploration importance for SMS study. It enables the determination of the time of onset and termination of mineralization which is defined by tectono-magmatic processes. Tectono-magmatic processes could provide a heat source and permeability of host rocks for fluid circulation and massive sulfides deposition during the active stage. Conversely, the heat deficit and/or lowering of permeability of host rocks result in termination of the hydrothermal mineral-forming process. Thus, the dating of sulfide deposits enables the reconstruction of tectono-magmatic processes as a whole and hydrothermal venting and SMS accumulation in particular. The last aspect has exploration importance (e.g. the age data can be used for resource estimation of SMS deposits).

Further discussion of fundamental and exploration issues is considering below based on dating of SMS deposits from the northern equatorial (NEq) part of the MAR.

The hydrothermal mineralization of the NEq MAR within the segment between 10° and 20°N has been studied by Russian geologists during numerous cruises of RV Professor Logatchev executed by Polar Marine Geosurvey Expedition and VNIIOkeangeologia (St. Petersburg, Russia) (Cherkashev et al., 2013). As a result, 18 hydrothermal fields with SMS deposits have been discovered. Some groups of closely located fields have been united as SMS clusters and now, 11 sites (fields and clusters) with SMS deposits are known within the area (Fig. 1).

The first age data for SMS samples recovered at the NEq MAR in 1994 at 14° 45′N (Logatchev field) were obtained (Lalou et al., 1996). The systematic determination of SMS age from other hydrothermal fields started in early 2000s at the St. Petersburg State University and is ongoing. During this time period, a large collection of massive sulfides from all known SMS deposits at the NEq MAR have been dated. Some data for separate hydrothermal fields have been published in Russian (Kuznetsov et al., 2007, 2013 – see Table 1) and just for three of them (Logatchev, Semenov and Peterburgskoye) in English (Kuznetsov et al., 2006, 2011, 2015).

We present here new dates for the Surprise, Pobeda, Semenov-5 and partly for the Peterburgskoye hydrothermal fields and review for all known deposits at the NEq MAR and adjacent area.

2. Geological setting and characteristic of deposits

NEq part of the MAR between 10° and 20° N is a typical slow spreading ridge segment which is characterized by a deep, fault-bounded axial valley with rift floor from 1.5 to 13 km wide and valley walls from 0.8 to 2.5 km high. Full spreading rate is estimated as 2.4 to 2.5 cm/year (DeMetz et al., 1990; Fujiwara et al., 2003). Three transform faults (Kane, Fifteen-Twenty and Marathon) divide the MAR into second order segments. The next (third) level is expressed by the occurrence of 24 segments with lengths from 13 to 72 km divided by non-transform discontinuities (Fig. 1).

Based on the mode of accretion and type of hosted rocks, two geological settings of SMS deposits at slow-spreading ridges are identified: symmetrical mode of accretion with basalts and asymmetrical accretion with gabbro-peridotites (Escartın et al., 2008). The same division of the MAR as a typical slow-spreading ridge is describing by other terms as "magmatic" (with domination of volcanic processes) and "tectonic" segments where magmatism is reduced and tectonics prevails. Half of the SMS deposits at the studied NEq of the MAR are associated with basalts (magmatic segments) and the other half with tectonic segments, with uplifted lower crust and mantle rocks (oceanic core complex – OCC) (Table 1). OCC is tectonically uplifted along detachment faults, which

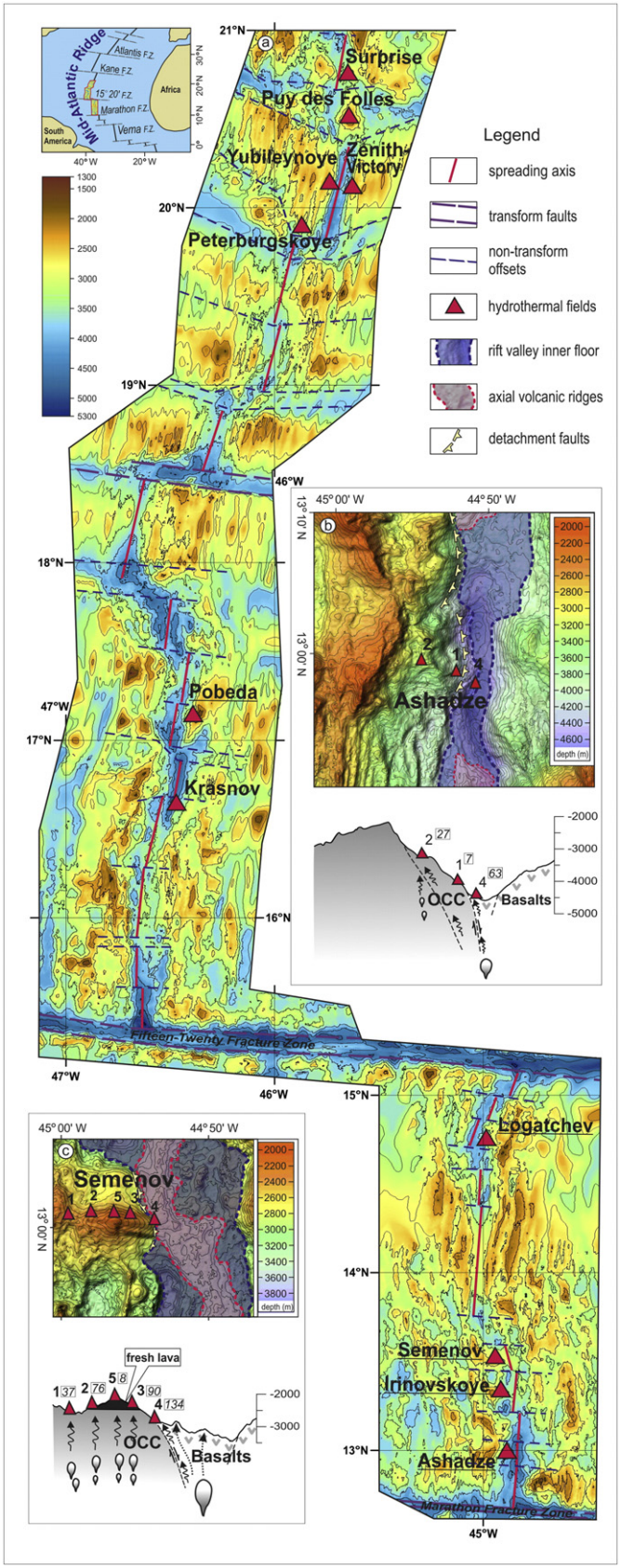

Fig. 1. Location of SMS deposits at the Northern Equatorial part of the Mid-Atlantic Ridge (a). Underlined – ultramafic-hosted deposits. (b) and (c) – detailed maps and cross-section for Ashadze and Semenov hydrothermal fields. Numbers in squares – age (ka).

Table 1
The parameters of the SMS deposits within the NE MAR. B – basalts; G-P – gabbro-peridotites. A – active, N – inactive, A (?) – hydrothermal activity expected on the basis of anomalies in the near-bottom waters; — no data. References in brackets: 1 – Kuznetsov and Maksimov (2012); 2 - Cherkashev et al. (2013); 3 – Kuznetsov et al. (in press); 4 - Kuznetsov et al. (2011); 5 - Kuznetsov et al. (2015); 6 - Kuznetsov et al. (2013); 7 - Kuznetsov et al. (in press); 8 – Lalou et al. (1996); 9 - Lalou et al. (1990); 10 - Lalou et al. (1993); 11 - Lalou et al. (1998b); 12 - Kuznetsov et al. (2006).

Deposit	Latitude, N	Distance from axis, km	Hosted rocks	Surface area of ore bodies, km^2	Hydrothermal activity	Minimal/maximal age, ka	Number of dated samples [reference]
Ashadze-1	12°58′	2.9	G-P	0.01	A	0–~7.2	8 [1]
Ashadze-2		7.6	G-P	0.06	A	0–~27	15 [1]
Ashadze-4		1.4	B	–	N	63.5 ± 10.8	1 [2]
Irinovskoye	13°20′	4	G-P	0.09	A	~7.8–~69	11 [3]
Semenov-1	13°30′	10.5	G-P	0.07	N	~13–~37	7 [4]
Semenov-2		8	G-P	0.15	A	~3.1–~76	7 [4]
Semenov-3		3.5	G-P	–	N	~36–~90	5 [4]
Semenov-4		0.5	B	0.28	N	~1.7–~124	19 [4]
Semenov-5		5	G-P	–	N	~8.0	2 [new data]
Logatchev-1	14°45′	7.5	G-P	0.04	A	0–~58	14 [1]; 16 [8]
Logatchev-2		11.5		0.01	A	~3.9–~7.0	2 [1]
Krasnov	16°38′	8	B	0.16	N	~5.6–~119	21 [1]
Pobeda	17°08′	8.2	G-P	0.19	A (?)	0–~177	16 [new data]
Peterburgskoye	19°52′	16	B	0.06	N	~63–~223	10 [5]; 8 [new data]
Zenith-Victory	20°07′	8	B	0.52	A (?)	~0.5–~60	25 [6]
Yubileynoye	20°08′	8	B	0.095	N	~2.6–~101	24 [7]
Puy des Folles	20°30′	0	B	0.85	A (?)	~2.2–~18	10 [new data]
Surprise	20°45′	1.5	B	–	N	~79–~102	2 [new data]
Snakepit	23°22′	0	B	–	A	~0.5–~3.7	3 [9]; 13 [10]
TAG (Active mound)	26°08′	2.4	B	0.03	A	~2–~20	14 [11]
Rainbow	36°13′	6	G-P	–	A	~2–~23	4 [12]

exhume in the footwall deep-seated gabbro-peridotite rocks onto the seafloor and may provide pathways for hydrothermal fluids (Smith et al., 2006; MacLeod et al., 2009). Two examples of OCC related SMS deposits (Ashadze and Semenov) are shown on Fig. 1(b) and (c). Hydrothermal fields within Semenov and Ashadze clusters are situated both with footwall OCC gabbro-peridotites (Ashadze-1, 3 and Semenov 1–3, 5) and hanging wall basalts (Ashadze-4 and Semenov-4).

The water depth of SMS deposits varies from 1940 m (Puy des Folles) to 4350 m (Ashadze-4) with average 2700 to 2800 m being close to the mean water depth of SMS in the ocean (Hannington et al., 2005).

The hydrothermal accumulations have a hierarchy based on the scale of their occurrence. The first level is the SMS body that is represented by continuous sulfide deposit. The hydrothermal field may include several sulfide ore bodies as well as adjacent ferromanganese crusts and metalliferous sediments that are dispersed and accumulated around vents and chimneys. In places, closely spaced hydrothermal fields are considered as SMS clusters.

SMS deposits along the NEq MAR are usually isometric (or close to isometric) in 2D dimension whereas their 3D morphology depends on the geological environment. As it was shown by Fouquet et al. (1993) in ultramafic environments, the discharge is clearly less focused than at basaltic sites. This “diffuse” discharge through more permeable hydrothermally altered ultramafic rocks produces relatively flat-lying deposits without clearly organized mounds. The latter are quite different from basaltic environments where conical mounds are typically formed (Fig. 2). Morphology of two types of deposits is important for estimating their volume and will be consider in further discussion regarding age-resources relations at the NEq MAR (Section 5.5).

The minerals forming SMS deposits include iron sulfides such as pyrite, as well as the main minerals of economic interest such as chalcopyrite (copper sulfide) and sphalerite (zinc sulfide). The precious metals

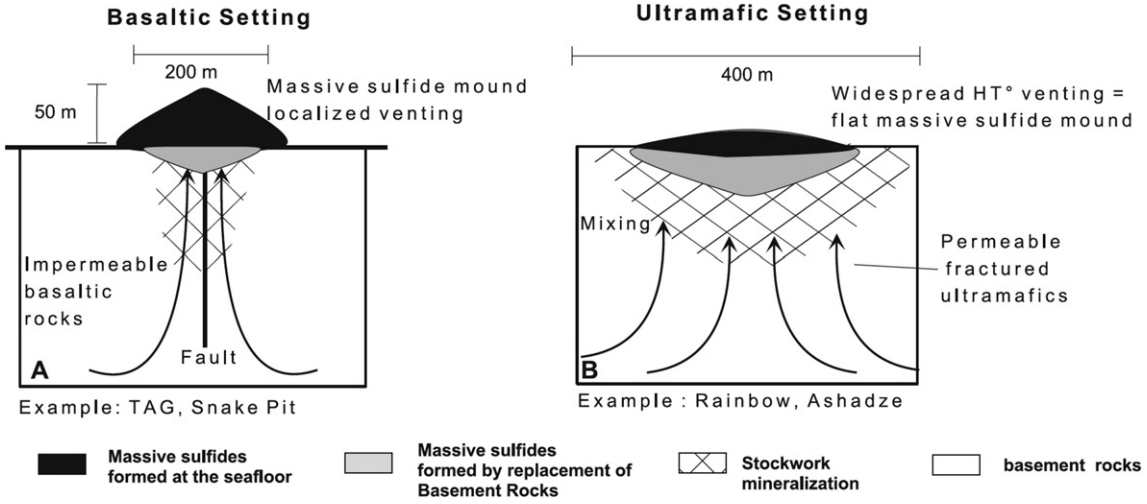

Fig. 2. Differences in the morphology of deposits and type of discharge between basalt- and ultramafic-hosted hydrothermal deposits. Compared to (A) basalt hosted fields, discharge is less focused in (B) ultramafic environments, and no clear mound structures formed (Fouquet et al., 2010).

gold and silver may also occur in elevated concentrations, together with non-sulfide (gangue) minerals, which are predominantly sulfates, carbonates and silicates. Mineralogy and chemistry of SMS depend on the nature of basement rocks affected by hydrothermal circulation, the water depth, the phase separation processes, and the maturity of deposits (Hannington et al., 2005).

3. Samples and methods

194 samples dated were collected during numerous cruises of the RV Professor Logatchev from 18 hydrothermal fields. The number of samples collected from particular hydrothermal fields varied from 1 (Ashadze-4) to 24 (Zenith-Victory), averaging 11 (Table 1). All samples were recovered by dredge and TV grabs from the surface of mineralized bodies. There are no drill core samples from the area. Taking into account the sampling methods, the geochronological data could be considering as a first approximation and we will get more detailed data when the inner parts of ore bodies are drilled.

The composition of the samples reflects a wide spectrum of mineralogical and geochemical types of SMS at the NEq MAR.

3.1. Ages of sulfide samples were determined using the ^{230}Th/U method

The geochemical-radiometric system used for ^{230}Th/U dating is as follows. A high-temperature hydrothermal fluid discharged at the seafloor has low U concentrations almost two orders less than ambient seawater (ca. 0.06–0.15 ppb (Lalou et al., 1996) and ca. 3.22 ppb respectively (Chen et al., 1986)). During mixing of the fluid with seawater, the dissolved uranyl-carbonate complexes transform into absorbable uranyl or poorly soluble U^{IV} ions. The latter co-precipitates with particles of transition metal sulfides from the fluids (Lalou and Brichet, 1987; Kuznetsov et al., 2006). By this process, uranium (without its daughter nuclide ^{230}Th) accumulated in the SMS deposits on the seafloor. Common uranium concentrations in SMS deposits range up to a few tens of ppm (Lalou et al., 1996; Kuznetsov et al., 2006; Kuznetsov and Maksimov, 2012). Decay of U and daughter products gives rise to accumulation of ^{230}Th with time. Hence, to determine an age of these deposits it is necessary to know the present-day ^{230}Th/^{234}U activity ratio (AR). The main theoretical prerequisites of the ^{230}Th/U-method for massive sulfide dating and their application are presented by Lalou and Brichet (1987), Lalou et al. (1996), Kuznetsov et al. (2006, 2007), Kuznetsov et al. (2012), Kuznetsov and Maksimov (2012), and Ditchburn et al. (2012).

For U and Th analysis, 2 to 4 g of sample was dissolved in a mixture of HCl-HNO_3 concentrated acids (Aqua Regia) before a precisely weighed quantity of a spike (^{228}Th-^{232}U at equilibrium) is added. The non-soluble insignificant residue (no >3–5% of sample mass) was removed by centrifugation. The U and Th fractions were purified and separated by applying anion exchange. Anionite resin AV-17 is used to capture the U and Th fractions both dissolved in a 7 N HNO_3. The U and Th isotopes are then eluted separately using 8 N HCl and a mixture of HNO_3 and HCl (0.5 N HNO_3, 1 N HCl), respectively. The separated U and Th fractions are finally purified by repeated anion exchange in micro-columns under the same conditions. After that, they are electrochemically deposited on separate platinum discs from the ethyl alcohol solution (adding a 0.2 N HNO_3 solution) during 1.5 h under current density of 60 mA/cm^2 for α counting. The specific ^{238}U, ^{234}U, ^{232}Th, and ^{230}Th activities are measured over several days applying the alpha-spectrometer "Alpha Duo" (ORTEC).

Then, the ^{230}Th/U age of a sample was derived with 1σ standard deviation (Kaufman and Broecker, 1965):

$$^{230}\mathrm{Th}/^{234}\mathrm{U} = (1-e^{-\lambda o t})/\gamma + (1-1/\gamma)\cdot(\lambda_o/(\lambda_o-\lambda_4))\cdot\left(1-e^{-(\lambda o-\lambda 4)t}\right), \quad (1)$$

where: ^{230}Th - specific activity of radiogenic ^{230}Th; ^{234}U - specific activity; γ - ^{234}U/^{238}U AR;

λ_o and λ_4 are the ^{230}Th and ^{234}U decay constants respectively, t - is the age of the sample.

The specific ^{232}Th activity was very low in some samples, even below the detection limit in most of the analyzed samples. These data indicate the absence of SMS samples contamination by terrigenous material and correspond to the requirements of the ^{230}Th/U dating method. Sample 107-9 from the Pobeda field was not datable because it had ^{230}Th/^{234}U AR >1.0. Samples 204-4 (from the Pobeda field), 159 and 159a (from the Peterburgskoye field) were not datable because their ^{238}U, ^{234}U and ^{230}Th specific activities were close to the detection limit. For the same reason the estimated age of ≤15.6 ka was obtained for the sample 242 (from the Semenov-5 field).

4. Results

All dates available for the NEq MAR, which include the earlier published data and new results for SMS from hydrothermal fields Pobeda (16 samples), Surprise (2 samples), Semenov-5 (2 samples) and additional age determinations of Peterburgskoye (8 samples), are presented in Supplement Table S1 and Fig. 3.

Generalized geochronological data and some characteristics of each field, including the state of hydrothermal activity, location (distance from the spreading axis), type of host rocks and mapped area of deposits on the sea floor are presented in Table 1. The data for the closely situated hydrothermal fields Snakepit, TAG and Rainbow are included as well. The relations of all listed parameters with SMS ages will be discussed below.

The following SMS with maximum ages <25 ka can be assigned to the group of relatively young deposits (ka): Snakepit (4.2), Logatchev-2 (7.0), Ashadze-1 (7.2), Semenov-5 (8.0), Puy des Folles (18.0), Active Mound at the TAG (20), and Rainbow (23). Another group with relatively old maximum ages (exceeding 100 ka) includes Yubileynoye (101.2), Surprise (101.7), Krasnov (119), Semenov-4 (123.8), Pobeda (177.5), and Peterburgskoye deposits. The newly obtained data for Peterburgskoye field confirms its oldest age, with the maximum age of 223 ± 38 ka. All the other fields have intermediate ages from 27 ka (Ashadze-2) up to 90 ka (Semenov-3). An average maximum age of all the hydrothermal fields within the NEq MAR is 66.1 ka.

Among all dated SMS deposits, about half are presently active systems and half are inactive fields. It should be noted that among the active fields the youngest ages tend to be very close to zero, which indirectly confirms the representation of the collected samples and the accuracy of dates.

SMS deposits within the area are located at varying distances from the spreading axis – from zero (Puy des Folles, Snakepit) to 16 km (Peterburgskoye) and are hosted either by basaltic or by ultramafic rocks almost in equal proportions.

The surface area of the ore bodies was estimated visually by video profiling from the deep-towed sledge. Having no drilling data, this parameter was used as the best available proxy for estimation of the volume of mineralized mass accumulated during the process of hydrothermal activity (see Section 5.5).

5. Discussion

5.1. SMS age at different spreading rates of the mid-ocean ridges

The differences in parameters and processes on mid-ocean ridges with fast, intermediate and slow spreading rates include varieties in age assessment of sulfide mineralization. Thus, sulfide age on the fast (EPR) and intermediate (Juan de Fuca Ridge) does not exceed 10 ka (Lalou and Brichet, 1982; Jamieson et al., 2013), whereas the average age of samples from the 18 fields on the NEq MAR is 66.1 ka, with a significant number of samples dated at 100 ka and older. The SMS deposit

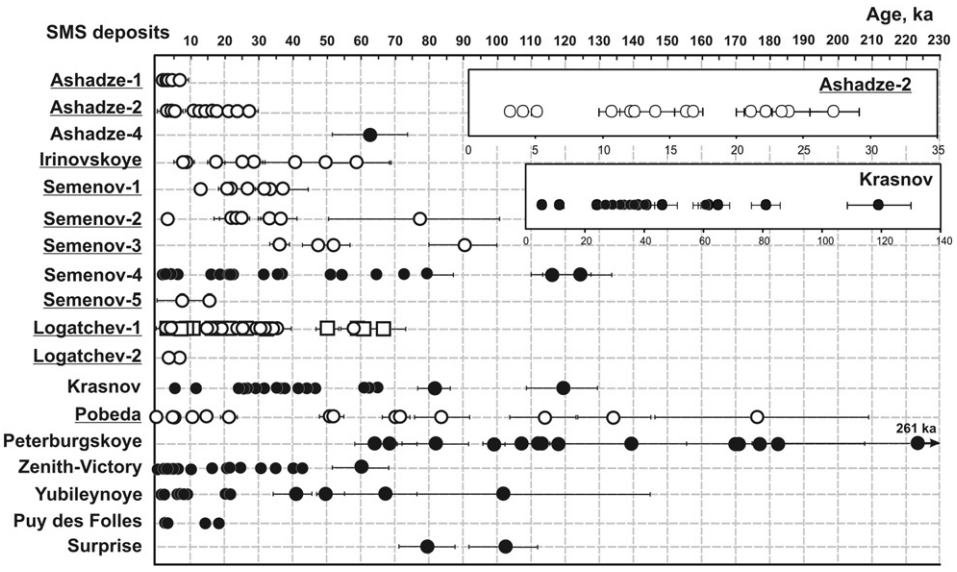

Fig. 3. Dating results with the 1σ variability for SMS deposits at the NEq MAR. Circles – our data (filled circles – basalt–hosted, empty circles – ultramafic-hosted deposits), empty squares – data from Lalou et al. (1996).

of Peterburgskoye hydrothermal field with an age of 223 ± 38 ka is the oldest within the MAR (Table 1). Such age differences might be attributed to very intense volcanic activity with frequent and extensive lava flows overlaying older sulfide deposits at fast and intermediate spreading ridges (older SMS may exist but are buried). For the older (and larger) deposits to be preserved on the seafloor of fast-spreading ridges, they must have formed away from the axial zone of the EPR, at off-axial volcanoes where the possibility to be buried by lava flows is unlikely (Fouquet et al., 1993).

The short time-scales of hydrothermal discharge (only 10s to 1000s of years) result in formation of small deposits on intermediate and fast spreading ridges (Lalou et al., 1985; Jamieson et al., 2013). On the contrary, long-lived hydrothermal circulation and discharge on the slow-spreading MAR are a major factor in the large size of the deposits. The favorable conditions for producing long-lived hydrothermal systems are provided by deep-seated magmatic activity followed by long periods of cooling and release of heat from depth. Reduced volcanism could be considered as additional factor to preserve SMS outcrops on the surface of slow-spreading ridges. Relations between size and age of deposits within the NEq MAR will be considered further.

5.2. Active and inactive hydrothermal fields

Data on age combined with direct visual observations make it possible to evaluate present-day activity of hydrothermal fields. Analysis of the data for 18 sites (Table 1) demonstrates that the number of inactive fields (9) exceeds the number of active fields (6). In the remaining three fields hydrothermal activity was not visually recorded, but hydrothermal activity was suggested by the presence of anomalies in the near bottom waters.

The conclusion regarding equal numbers of active and inactive sites is very important not only from a scientific point of view, but also from the practical point of view, taking into account environmental aspects of the potential mining of SMS deposits with and without hydrothermal biological communities at the active and inactive sites respectively.

Another observation is connected with estimating the age of the final period of inactivity, which was as old as 63 ka for the Ashadze-4 and Peterburgskoye sites and 79 ka for the Surprise site. This long period of inactivity demonstrates that old inactive SMS deposit can survive being in an oxidized environment for a long period of time.

5.3. Timing and periodicity of hydrothermal processes

The SMS dates show that hydrothermal venting events are distributed unevenly through the time interval from 250 to 1 ka. The distribution of events at all hydrothermal fields (Fig. 4A) demonstrates that maximum activity occurred at 38–35, 30–20, and 8–2 ka and the number of events was fewest during the older period of time. This gradual increase of activity with time can characterize natural evolution of hydrothermal systems. It also could have been a result of either incomplete sampling of the older deposits or of natural destruction of older sulfide edifices (buried by lava flows?). Apart from sulfide dating, important information of chronology and the development of hydrothermal systems can be obtained from examination of sedimentary cores next to the hydrothermal fields owing to a continuous record of changes in conditions under which the systems evolved. Joint analyses of the sediment cores and SMS will provide an added dimension to our understanding of the hydrothermal systems (Shilov et al., 2012; Kuznetsov et al., in press).

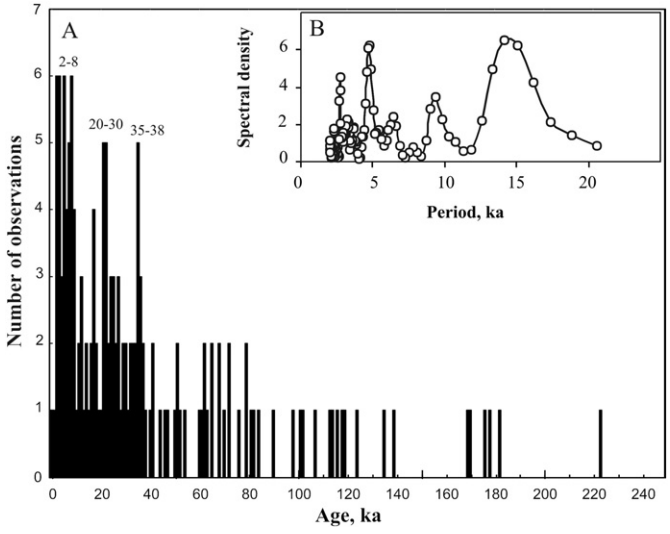

Fig. 4. A - Distribution bar chart of hydrothermal events (N = 163) for last 250 ka interval determined by ^{230}Th/U dating of SMS deposits. B - Spectral density vs. period spectrum of hydrothermal events with marked physically and statistically significant peaks at 15, 9 and 5 ka periods.

Episodicity is a typical feature of hydrothermal systems: active and inactive periods of the SMS formation alternate (Fig. 3). The distribution of sulfide ages at the Ashadze-2 and Krasnov fields shows 3 to 5 distinct periods of hydrothermal activity (inset of Fig. 3). However, this visual method of determining episodes has a subjective character. In order to obtain more objective results, spectral statistical analysis of time series initial data, after exponential smoothening, was performed using the program Statistica 8.0. StatSoft, Inc. (2007). The SMS generation spectra depicted in Fig. 4B show a major spectral density peak at 14.1 ka. Additional minor peaks are seen at 9.4 and 4.7 ka, which are statistically and geologically meaningful values. Three time intervals are most likely for the periodicity of deposit formation for the entire study area: 4.7, 9.4 and 14.1 ka.

As for the global geological control of hydrothermal activity periodicity, recent publications (e.g. Lund et al., 2016; Middleton et al., 2015) demonstrated that intervals of intense hydrothermal activity on the EPR and MAR occurred during the last two glacial terminations. Based on these observations, it was proposed that there may be a direct causal relationship between sea-level rise and hydrothermal activity. Taking into account that the last glacial maximum occurred from 30 to 25 ka (Clark et al., 2009), part of our data support this relationship for the NEq MAR as well. However, reasons for two other maxima of hydrothermal activity observed in the studied area (38–35 and 8–2 ka) are still problematic.

5.4. Correlation between age and location of SMS deposits

Fig. 5 is plot of ages versus location of SMS deposits. The location (distance between hydrothermal field and ridge axis) was estimated for both types of SMS mentioned above. The two types show clear differences: a positive correlation exists for basalt-hosted deposits and there is no correlation for the gabbro-peridotite-hosted hydrothermal systems. This difference may suggest that formation of basalt-hosted deposits was related to the axial magma chamber whereas gabbro-peridotite-hosted system moved away from the rift valley according to a "classical" spreading geodynamic model. The oldest known hydrothermal field is Peterburgskoye, which is situated on basalts and located 16 km away from the spreading axis of the MAR. A similar trend with progressive aging of sulfide deposits from the center to the margins of the axial valley has also been observed at the Endeavour segment of the intermediate-spreading rate Juan de Fuca Ride (Jamieson et al., 2013).

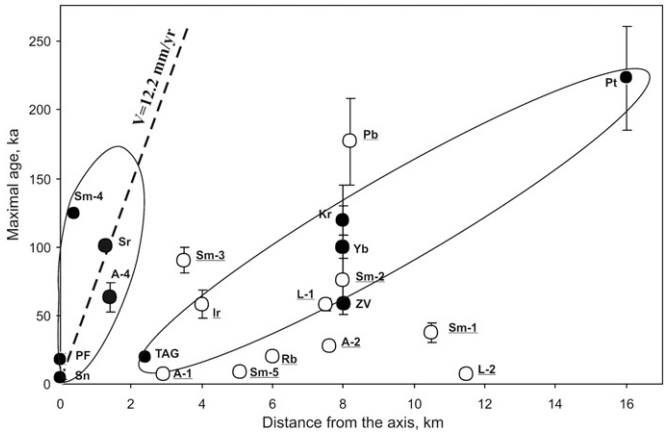

Fig. 5. Relationship between distance from the spreading axis vs. age of the SMS deposits. Dotted line shows linear correlation between the two parameters for an average half-spreading rate 12.2 mm/year (Fujiwara et al., 2003). Left field encloses basalt-hosted deposits that follow this trend. Abbreviations: Sn – Snakepit, PF – Puy des Folles, A – Ashadze, Sr – Surprise, Sm – Semenov, Ir – Irinovskoye, Rb – Rainbow, L – Logatchev, Yb – Yubileynoye, Kr – Krasnov, Pb – Pobeda, Pt – Peterburgskoye.

Some basalt-hosted fields (Snakepit, Puy des Folles, Ashadze-4, Surprise and Semenov-4) lie close to the line representing the average half-spreading rate for the NEq MAR (12.2 mm/year, Fujiwara et al., 2003). From this observation we infer that they originated very close to the axis and then moved away as a result of the spreading. Other basalt-hosted fields (TAG, Krasnov, Yubileynoye, Zenith-Victory and Peterburgskoye) lay away from the main trend, apparently because they formed at some distance from the spreading axis. Taking into account the value of 12.2 mm/year as an average half-spreading rate for this MAR segment, we calculate the precise location of origin for these hydrothermal fields. The result shows that the initial distance from the axis varies from 2 km for TAG to 13 km for Peterburgskoye.

A different situation arises with deposits related to deep-seated rocks. For those deposits, there is no correlation between the distance from the spreading axis and the age of the hydrothermal system. This reflects a different mechanism of formation under conditions of asymmetric accretion for which the activation of hydrothermal processes might not have been controlled by the influence of the axial magmatic chamber. Rather, the heat source was the intrusion of gabbroic magma into the rocks of the oceanic core complex, which took place during different time intervals at different distances from the ridge axis. Such a distribution is recorded, in particular, for the Semenov deposits, where an older SMS field changes to a younger one at the footwall of the detachment at the oceanic core complex surface with increase in distance from the ridge axis (Fig. 1c). Deposits located on the hanging wall of the detachment, Ashadze-4 and Semenov-4, represent a special case (Fig. 1b and c). The basalt-hosted sulfides close to axial zone 1.4 and 5.1 km are rather old, 63.5 ka and 124 ka, respectively. The SMS-forming mechanism that could lead to such old deposits near the axial zone is still unclear.

5.5. Correlation between age and resources of SMS deposits at the NEq MAR

Taking into account the duration of ore precipitation it was expected that older deposits should have larger tonnage/size. This correlation was confirmed by comparing EPR and MAR deposits: long-lived MAR hydrothermal systems produce larger accumulations of sulfides than younger systems at the EPR (Section 5.1). We have tried to compare age and size for deposits of the NEq MAR as well. As mentioned above, there are no available data for the third dimension of these deposits due to the lack of drilling operations or high-resolution mapping that would allow for the calculation of deposit volumes (Jamieson et al., 2014). Because of this, the distribution area of the ore bodies (Table 1) was considered as the best available proxy to evaluate deposit volume.

The total area of ore bodies within each hydrothermal field was calculated using ArcGIS 10.4 software. The statistical analyses of SMS body area and age shows a direct positive correlation for deposits related to ultramafic-hosted systems and no correlation for basalt-hosted deposits (Fig. 6). The reason of this difference could be connected with difference of SMS body morphology related to basalt or ultramafic environments. According to the model described above (Section 2), deposits associated with ultramafic rocks should have a more flat-lying profile whereas mound-like structures are more typical for basalt-hosted deposits (Fouquet et al., 1993). The area of flat-lying SMS bodies provides for a better approximation of the volume/resource than the same parameter for the mound-like structure.

Future resource evaluation through drilling will provide the data required to determine the efficacy of this idea. However, the age data can be used to estimate resources of SMS deposits and research of small SMS bodies with great ages should be continued considering extension of their volume/tonnage.

6. Conclusions

Geochronological studies using the ^{230}Th/U technique have been completed for 194 samples of massive sulfides from 18

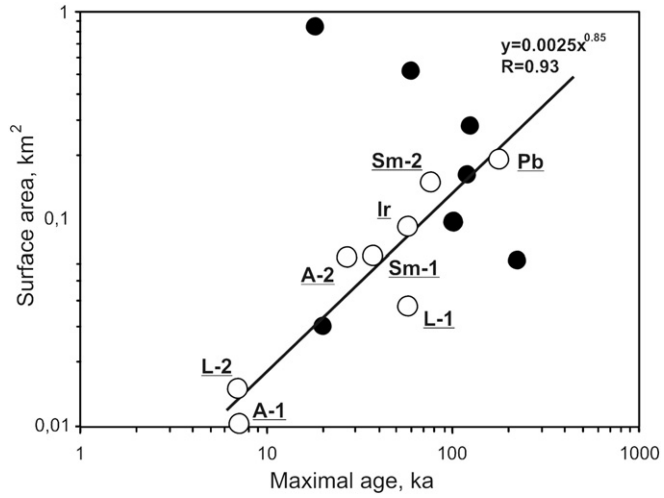

Fig. 6. Relationship between age and estimated surface area of the deposits. Filled circles – basalt–hosted, empty circles – ultramafic-hosted deposits. For the latter group, a strong correlation is observed between age and surface area. Abbreviations are the same as for Fig. 5.

hydrothermal fields of the slow spreading Northern Equatorial Mid-Atlantic Ridge. The ages range from 223 to 0 ka with the average age 66.1 ka. The SMS deposit of Peterburgskoye hydrothermal field with the age 223 ± 38 ka is the oldest age measured along the MAR. Data obtained confirm that hydrothermal processes at slow-spreading ridges have a long-lived character resulting in accumulation of large deposits opposed to the small relatively young deposits formed at intermediate and fast spreading Pacific mid-ocean ridges. Longer-lived systems produced larger volume hydrothermal SMS deposits at the regional level as well: older SMS within the NEq MAR have wider areas of distribution compared with younger ones. It was confirmed based on statistical analyzes for the flat-lying profile deposits related to the ultramafic-host environment. Thus, age data allow for the estimation of volume of deposits and this aspect could have an exploration importance.

Two types of SMS deposits at the slow-spreading ridges associated with magmatic- or tectonic- dominated segments (basalt or ultramafic-host rocks) are characterized by different genetic processes and statistics show correlations between the age and distance from the axial rift zone as well as between the age and area of the deposits.

The SMS formation process exhibits a discrete pattern reflected in the alternation of active and inactive stages. The distribution of events demonstrates that maximum activity over the entire area occurred from 38 to 35, 30 to 20, and 8 to 2 ka and increased with time. The second period (30–20 ka) is close to the Last Glacial Maximum, which is proposed as a time of lowest sea level that resulted in intense hydrothermal activity (Lund et al., 2016).

The geochronological analysis of hydrothermal systems is of both fundamental and implied importance, which warrants further investigations and studies of the SMS deposits formation.

Supplementary data to this article can be found online at doi:10.1016/j.oregeorev.2016.10.015.

Acknowledgements

This study was supported by projects 3.37.135.2104 and 18.37.141.2014 of St. Petersburg State University. GC wishes to thank Irina Poroshina for her assistance with preparation of Fig. 1.

We deeply thank the editor of Special Issue Dr. James Hein and two reviewers for the very substantial and helpful comments and recommendations that greatly improved this paper.

References

Chen, G.J., Wasserburg, K.L., von Damm, K., Edmond, J.M., 1986. The U-Th-Pb systematic in hot springs of the East Pacific Rise at 21°N and Guaymas Basin. Geochim. Cosmochim. Acta 50, 2467–2479.

Cherkashev, G.A., Ivanov, V.N., Bel'tenev, V.I., Lazareva, L.I., Rozhdestvenskaya, I.I., Samovarov, M.L., Poroshina, I.M., Sergeev, M.B., Stepanova, T.V., Dobretsova, I.G., Kuznetsov, V.Yu, 2013. Massive sulfide ores of the northern equatorial Mid-Atlantic Ridge. Oceanology 53 (5), 607–619.

Clark, P.U., Dyke, A.S., Shakun, J.D., Carlson, A.E., Clark, J., Wohlfarth, B., Mitrovica, J.X., Hostetler, S.W., McCabe, A.M., 2009. The Last Glacial Maximum. Science 325 (5941), 710–714.

de Ronde, C.E.J., et al., 2011. Submarine hydrothermal activity and gold-rich mineralization at Brothers Volcano, Kermadec Arc, New Zealand. Mineral. Deposita 46 (5–6), 541–584.

Delaney, J.R., McDuff, R.E., Robigou, V., Schultz, A., Smith, M., Wells, J., Atnipp, V., McClain, J., 1990. Covariation in microseismicity and hydrothermal output in the Endeavour vent field. Eos Trans. AGU 71, 1609.

DeMetz, C., Gordon, R.G., Argus, D.F., Stein, S., 1990. Current plate motions. Geophys. J. Int. 101, 425–478.

Ditchburn, R.G., de Ronde, C.E.J., Barry, B.J., 2012. Radiometric dating of volcanogenic massive sulfides and associated iron oxide crusts with an emphasis on ^{226}Ra/Ba and ^{228}Ra/^{226}Ra in volcanic and hydrothermal processes at intraoceanic arcs. Econ. Geol. 107 (8), 1635–1648.

Escartın, J., Smith, D.K., Cann, J., Schouten, H., Langmuir, C.H., Escrig, S., 2008. Central role of detachment faults in accretion of slow-spreading oceanic lithosphere. Nature 455, 790–795.

Fouquet, Y., Wafik, A., Cambom, P., Mevel, C., Meyer, G., Cente, P., 1993. Tectonic setting and mineralogical and geochemical zonation in the Snake Pit sulfide deposit (Mid-Atlantic Ridge at 23° N). Econ. Geol. 54, 2018–2036.

Fouquet, Y., Cambon, P., Etoubleau, J., Charlou, J.L., Ondréas, H., Barriga, F.J.A.S., Cherkashov, G., Semkova, T., Poroshina, I., Bohn, M., Donval, J.P., Henry, K., Murphy, P., Rouxel, O., 2010. Geodiversity of hydrothermal processes along the Mid-Atlantic Ridge and ultramafic-hosted mineralization: A new type of oceanic Cu-Zn-Co-Au volcanogenic massive sulfide deposit. In: Diversity of Submarine Hydrothermal Systems on Slow Spreading Oceanic Ridges. Geophysical Monograph 188, pp. 297–320.

Franklin, J.M., Gibson, H.L., Jonasson, I.R., Galley, A.G., 2005. Volcanogenic massive sulfide deposits. Economic Geology 100th Anniversary Volume, pp. 523–560.

Fujiwara, T., Lin, J., Matsumoto, T., Kelemen, P.B., Tucholke, B.E., Casey, J.F., 2003. Crustal evolution of the Mid-Atlantic Ridge near the Fifteen-Twenty Fracture Zone in the last 5 Ma. Geochem. Geophys. Geosyst. 4 (3), 1024.

Hannington, M.D., de Ronde, C., Petersen, S., 2005. Sea-floor tectonics and submarine hydrothermal systems. Economic Geology 100th Anniversary Volume, pp. 111–141.

Jamieson, J., Hannington, M., Clague, D., Kelley, D., Delaney, J., Holden, J., Tivey, M., Kimpe, L., 2013. Sulfide geochronology along the Endeavour Segment of the Juan de Fuca Ridge. Geochem. Geophys. Geosyst. 14, 2084–2099.

Jamieson, J., Clague, D., Hannington, M., 2014. Hydrothermal sulfide accumulation along the Endeavour Segment, Juan de Fuca Ridge. Earth Planet. Sci. Lett. 395, 136–148.

Kaufman, A., Broecker, W.S., 1965. Comparison of ^{230}Th and ^{14}C ages for carbonates materials from Lakes Lahontan and Bonneville. J. Geophys. Res. 70, 4030–4042.

Kelley, D.S., et al., 2012. Endeavour Segment of the Juan de Fuca Ridge: one of the most remarkable places on earth. Oceanography 25 (1), 44–61.

Kuznetsov, V.Yu, Maksimov, F.E., 2012. Geochronometrical Methods of the Quaternary Deposits in Paleogeography and Marine Geology. Nauka, SPb, p. 191 (in Russian).

Kuznetsov, V., Cherkashev, G., Lein, A., Maksimov, F., Arslanov, K., Stepanova, T., Chernov, S., Tarasenko, D., 2006. ^{230}Th/U dating of massive sulfides from the Logatchev and Rainbow hydrothermal fields (Mid-Atlantic Ridge). Geochronometria 26, 51–56.

Kuznetsov, V.Yu, Cherkashev, G.A., Bel'tenev, V.E., Lein, A.Y., Maximov, F.E., Shilov, V.V., Stepanova, T.V., 2007. The ^{230}Th/U dating of sulfide ores in the ocean: methodical possibilities, measurement results and perspectives of application. Dokl. RAS 417 (8), 1202–1205 (in Russian).

Kuznetsov, V., Maksimov, F., Zheleznov, A., Cherkashov, G., Bel'tenev, V., Lazareva, L., 2011. ^{230}Th/U chronology of ore formation within the Semyenov hydrothermal district (13°31′ N) at the Mid-Atlantic Ridge. Geochronometria 38, 72–76.

Kuznetsov, V., Cherkashov, G., Bel'tenev, V., Lazareva, L., Maksimov, F., Zheleznov, A., Baranova, N., Zherebtsov, I., Levchenko, S., Tabuns, E., 2012. ^{230}Th/U Chronology of Ore Formation within the "Zenith-Victory", "Peterburgskoe" and "Puy des Folles" Hydrothermal Fields (Mid-Atlantic Ridge). Abstract Volume "Minerals of the Ocean-6"VNIIOkeangeologia, St. Petersburg, Russia, pp. 113–114.

Kuznetsov, V.Yu, Tabuns, E.V., Bel'tenev, V.E., Cherkashov, G.A., Maksimov, F.E., Kuksa, K.A., Baranova, N.G., Levchenko, S.B., 2013. ^{230}Th/U chronology of the formation of deep-sea polymetallic sulfides within the «Zenith-Victory» hydrothermal field (20°08′ N), Mid-Atlantic Ridge. Vestn. SPSU 7 (4), 119–130 (in Russian).

Kuznetsov, V., Tabuns, E., Kuksa, K., Cherkashov, G., Maksimov, F., Bel'tenev, V., Lazareva, L., Zherebtsov, I., Grigoriev, V., Baranova, N., 2015. The oldest seafloor massive sulfide deposits at the Mid-Atlantic Ridge: ^{230}Th/U chronology and composition. Geochronometria 42 (1), 100–106.

Kuznetsov, V.Yu, Tabuns, E.V., Cherkashov, G.A., Bel'tenev, V.E., Maksimov, F.E., Kuksa, K.A., Lazareva, L.I., Levchenko, S.B., Zherebtsov, I.E., 2016a. ^{230}Th/U chronology and geochemistry of Irinovskoye hydrothermal ore field (Mid-Atlantic Ridge). Dokl. RAS (in press).

Kuznetsov, V.Yu, Tabuns, E.V., Kuksa, K.A., Cherkashov, G.A., Bel'tenev, V.E., Arslanov, K.A., Maksimov, F.E., Lazareva, L.I., Zhuravleva, A.I., Petrov, A.Y., Grigoriev, V.A., 2016b. Chronology of hydrothermal activity within the Yubileynoye ore field (Mid-Atlantic Ridge, 20°08′ N). Dokl. RAS (in press).

Lalou, C., Brichet, E., 1982. Ages and implications of East Pacific Rise sulphide deposits at 21°N. Nature 300, 169–171.

Lalou, C., Brichet, E., 1987. On the isotopic chronology of submarine hydrothermal deposits. Chem. Geol. 65, 197–207.
Lalou, C., Brichet, E., Hékinian, R., 1985. Age dating of sulfide deposits from axial and off-axial structures on the East Pacific Rise near 12°50′N. Earth Planet. Sci. Lett. 75, 59–71.
Lalou, C., Thomson, G., Arnold, M., Brichet, E., Druffel, E., Rona, P.A., 1990. Geochronology of TAG and Snake Pit hydrothermal fields, Mid-Atlantic Ridge: witness to a long and complex hydrothermal history. Earth Planet. Sci. Lett. 97, 113–128.
Lalou, C., Reyss, J.L., Brichet, E., Arnold, M., Thompson, G., Fouquet, Y., Rona, P.A., 1993. New age data for MAR hydrothermal sites: TAG and Snakepit chronology revisited. J. Geophys. Res. 98, 9705–9713.
Lalou, C., Reyss, J.L., Brichet, E., Krasnov, S., Stepanova, T., Cherkashev, G., Markov, V., 1996. Initial chronology of a recently discovered hydrothermal field at 14°45′N, Mid-Atlantic Ridge. Earth Planet. Sci. Lett. 144, 483–490.
Lalou, C., Munch, U., Halbach, P., Reyss, J.L., 1998a. Radiochronological investigation of hydrothermal deposits from the MESO zone, Central Indian Ridge. Mar. Geol. 149 (1–4), 243–254.
Lalou, C., Reyss, J.L., Brichet, E., 1998b. Age of sub-bottom sulfide samples at the TAG active mound. In: Herzig, P.M., Humphris, S.E., Miller, D.J., Zierenberg, R.A. (Eds.), Proceedings of the Ocean Drilling Program. Scientific Results vol. 158, pp. 111–117.
Lund, D.C., Asimow, P.D., Farley, K.A., Rooney, T.O., Seeley, E., Jackson, E.W., Durham, Z.M., 2016. Enhanced East Pacific Rise hydrothermal activity during the last two glacial terminations. Science 35 (6272), 478–482.
MacLeod, C.J., Searle, R.C., Casey, J.F., Mallows, C., Unsworth, M., Achenbach, K., Harris, M., 2009. Life cycle of oceanic core complexes. Earth Planet. Sci. Lett. 287, 333–344.
Middleton, J., Mukhopadhyay, S., McManus, J., Langmuir, C., 2015. Last glacial maximum and hydrothermal sediment fluxes on the Mid-Atlantic Ridge. Goldschmidt Abstr. 2123.
Münch, U., Lalou, C., Halbach, P., Fujimoto, H., 2001. Relict hydrothermal events along the super-slow Southwest Indian spreading ridge near 63856XE – mineralogy, chemistry and chronology of sulfide samples. Chem. Geol. 177, 341–349.
Shilov, V.V., Bel'tenev, V., Ivanov, V.N., Cherkashev, G.A., Rozhdestvenskaya, I.I., Gablina, I.F., Dobretsova, I.G., Narkevsky, E.V., Gustaitis, A.N., Kuznetsov, V.Yu, 2012. New hydrothermal fields at Mid-Atlantic Ridge: Zenith-Victory (20°08′ N) and Peterburgskoye (19°52′ N). Dokl. RAS 442 (3), 383–389 (in Russian).
Smith, D.K., Cann, J.R., Escartin, J., 2006. Widespread active detachment faulting and core complex formation near 13 N on the Mid-Atlantic Ridge. Nature 443, 440–444.
Wang, Y., Han, X., Jin, X., Qiu, Z., Ma, Z., Yang, H., 2012. Hydrothermal activity events at Kairei Field, Central Indian Ridge 25°S. Resour. Geol. 62 (2), 208–214.